

New perspective materials for solar cells: $\text{Cu}_2\text{CrSnS}_4$ solid solutions with orthorhombic structure

© M.V. Gapanovich^{1,2}, I.N. Odin⁴, I.M. Levin², V.V. Rakitin¹, D.M. Sedlovets³, G.V. Shilov¹, D.V. Korchagin¹

¹ Institute of Problems of Chemical Physics, Russian Academy of Sciences, 142432 Chernogolovka, Moscow region, Russia

² Moscow State University (Faculty of Fundamental Physical-Chemical Engineering), 119991 Moscow, Russia

³ Institute of Microelectronics Technology and High Purity Materials, Russian Academy of Sciences, 142432 Chernogolovka, Moscow region, Russia

⁴ Moscow State University (Chemical Faculty), 119991 Moscow, Russia

E-mail: gmw1@mail.ru

Received March 2, 2022

Revised March 24, 2022

Accepted March 24, 2022

The $\text{Cu}_2\text{CrSnS}_4$ microcrystalline powders and films with orthorhombic structure were obtained by solid-phase synthesis, and their Raman spectra were recorded for the first time. By optical spectroscopy, it was found that their $E_g = 1.70$ eV, while in energy band gap of the powders there is a donor level with $E = 1.23$ eV. It is shown for the first time that films of this material are photosensitive and have p -type of dark conductivity.

Keywords: solid-phase synthesis, microcrystalline powder, film, dark conductivity.

DOI: 10.21883/SC.2022.06.53544.9830

1. Introduction

Various quaternary copper compounds occupy a special place among the various semiconductors used to make the absorbing layer of solar batteries [1,2]. They also include compounds with a kesterite structure $\text{Cu}_{2-\delta}\text{ZnSnS}_{4-x}\text{Se}_x$ (CZTS(Se)). The elements within such materials are relatively low-toxic and, moreover, are widespread in nature. However, the efficiency of solar cells on their base at present does not exceed 13%. A number of authors think that this is due to the peculiarities of the structure of the given material, but this issue was not discussed in detail. One of the assumptions states that, due to the proximity of ionic radii of zinc Zn^{2+} and Cu^+ , many antisite defects Cu_{Zn} and Zn_{Cu} form in such a material and act as traps for photogenerated current carriers [3,4]. Substitution of ions in the cation sublattice of this material by ions with a radius, differing from the radius for Cu^+ , is of considerable scientific and practical interest. Thin films of $\text{Cu}_2\text{CrSnS}_4$ (CCrTS) can be used as such materials. Thus far there is only one paper describing the synthesis and properties of the given material [5], but it describes films with nanosized crystallites obtained by centrifuging. The properties of such specimens can differ from those of a bulk material.

Our paper describes the properties of microcrystalline powders and films of $\text{Cu}_2\text{CrSnS}_4$ obtained by solid-phase synthesis.

2. Experimental procedure

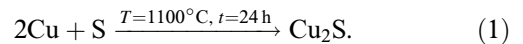
2.1. Materials

Copper (99.99%), tin (99.99%), chromium (99.97%) and sulfur (99.999%) were used for synthesis.

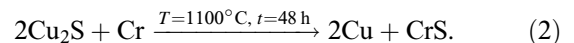
2.2. Synthesis of $\text{Cu}_2\text{CrSnS}_4$ polycrystalline powders

Synthesis was performed in several stages from metals Cu, Cr, Sn and elemental S in evacuated ($p_{\text{res.press.}} = 2 \cdot 10^{-3}$ mm Hg) quartz ampules.

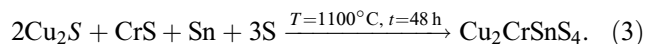
Cu_2S was obtained at the first stage:



Then the ampule was opened, its content was pulverized in an agate mortar and was again soldered up under vacuum with chromium quantity of which was calculated using response equation (2), and was annealed at $T = 1000^\circ\text{C}$ for 48 h:



Then the ampule was opened, its content was against soldered up together with tin and sulfur and annealed at $T = 1100^\circ\text{C}$ for 48 h:



Heating to the given temperatures was performed at the rate of 2 deg/min.

At the final stage, the ampule content was pulverized in an agate mortar for homogenization, then again soldered up under vacuum and annealed at $T = 600^\circ\text{C}$ for 1000 h.

The obtained substance was black ingots with metallic luster.

In order to synthesize CCrTS films, 155 nm of Cr, 345 nm of Sn and 300 nm of Cu were successively deposited onto a glass substrate and a glass/600 nm Mo substrate by thermal evaporation in deep vacuum ($P_{\text{res.press.}} = 8 \cdot 10^{-7}$ mm Hg). The obtained precursor films were soldered up in evacuated glass ampules with ~ 50 mg of SnS_2 . This compound, when heated in vacuum, disproportionates with formation of S and SnS vapors. S vapors sulfurize the precursor film, while SnS reduces the tin losses from the forming CCrTS film [6].

2.3. Specimen characterization

The phase composition of the obtained specimens was studied by a combination of XRF (PANalitical Aeris diffractometer, CuK_α emission) and Raman spectroscopy methods (Bruker Senterra micro-Raman system, 532 nm emission).

Reflection spectra were recorded on the Shimadzu UV-3101 PC spectrophotometer.

Cathode luminescence (CL) spectra were taken at 78 K. The specimens were excited by a pulsed electron beam with the energy of 40 keV. CL spectra were recorded using the DFS-13 monochromator. The procedure for taking of CL spectra is detailed in [7]. The error in determination of wavelength in the spectrum was ± 4 nm, and the error in photon energy calculation (we estimated the line maximum as ± 0.01 eV).

Photoconduction was studied by the photoelectrochemical cell method (PEC) [8–10]. The electrolyte was 0.2 M aqueous solution of $\text{Eu}(\text{NO}_3)_3$, the studied specimen acted as the working electrode. Shunt resistance was increased by insulating its edges with epoxy resin. The counterelectrode was a graphite rod, the reference electrode was 3 M Ag/AgCl . The light source was a metal halide lamp with the intensity of $0.1 \text{ W}/\text{cm}^2$.

3. Experimental results

3.1. Phase composition and structural data

Figure 1, *a* shows an X-ray image for the obtained powders. Crystallographic indices are given for the brightest lines.

It follows from the data of X-ray diffraction analysis (XRD) that the obtained powders have the structure of an orthorhombic space group Pmn_21 , lattice parameters $a = 6.28(9) \text{ \AA}$, $b = 8.32(8) \text{ \AA}$, $c = 6.17(16) \text{ \AA}$, $V = 322.7(71) \text{ \AA}^3$. The authors of [5] assume that the structure of $\text{Cu}_2\text{CrSnS}_4$ is tetragonal, space group is $I42 - m$, close to the one for CZTS kesterites. However, the X-ray image in this paper has only 4 lines, having a significant half-width since they pertain to nanoparticles. Thereat, it should be noted that their position in the diffractogram of

$\text{Cu}_2\text{CrSnS}_4$, given in [5], is close to the one for the bright lines in our figure.

Figure 1, *b* shows the diffractograms for out films depending on annealing time. The reference for $\text{Cu}_2\text{CrSnS}_4$ was the diffractogram for our powder. It can be seen from the figure that most lines in the diffractogram pertain

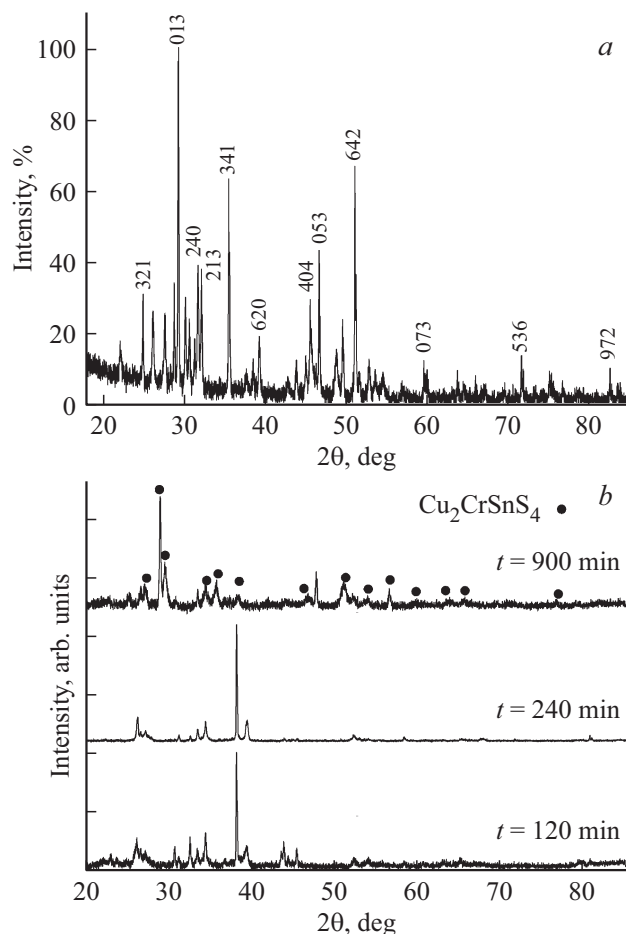


Figure 1. XRD data for the synthesized powders (*a*) and films (*b*).

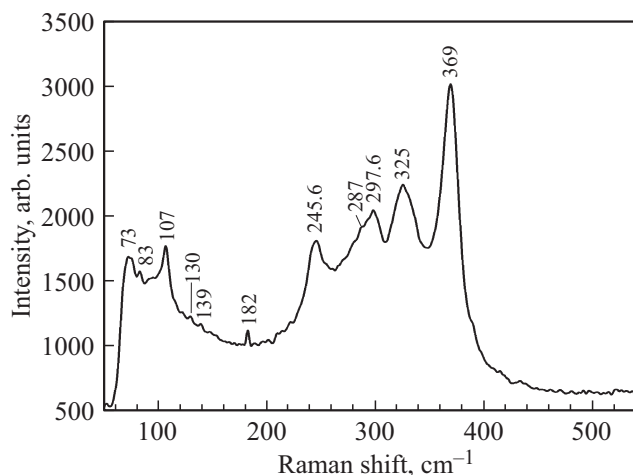


Figure 2. Raman spectrum for synthesized $\text{Cu}_2\text{CrSnS}_4$ powder.

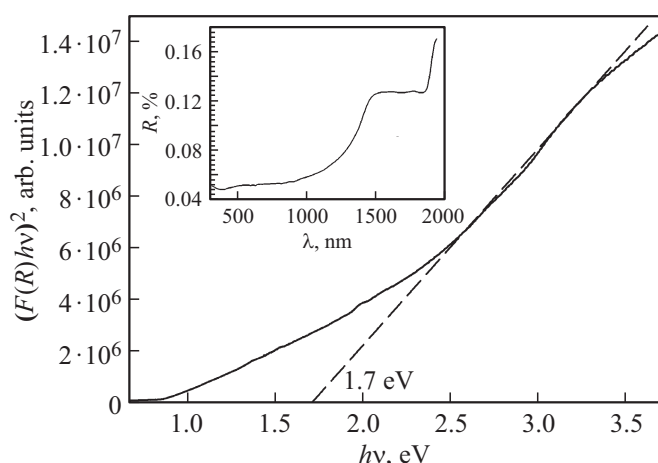


Figure 3. Absorption spectrum for the $\text{Cu}_2\text{CrSnS}_4$ film with annealing time $t = 900$ min in Tauc coordinates. The insert shows the reflection spectrum used for plotting.

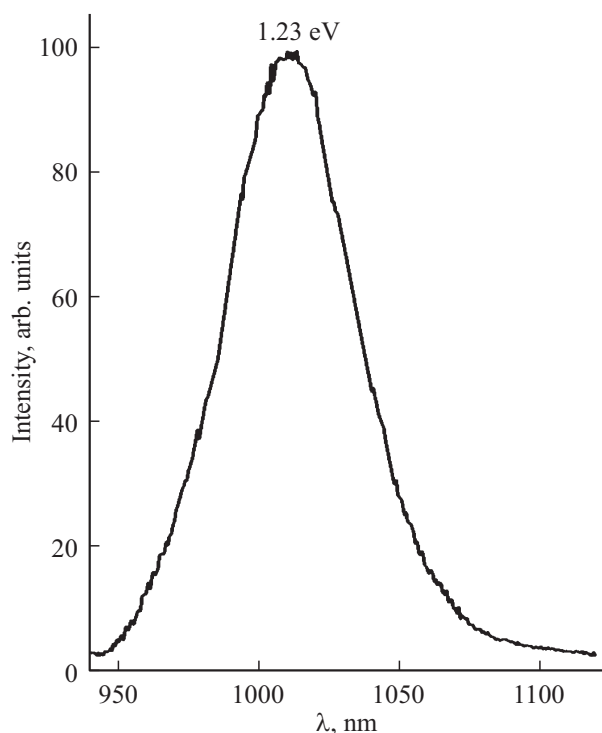


Figure 4. CL spectrum for $\text{Cu}_2\text{CrSnS}_4$ powder recorded at $T = 78$ K.

to $\text{Cu}_2\text{CrSnS}_4$ only for annealing time $t = 900$ min. The remaining films consist of other phases. These phases are copper, chromium and tin sulfides.

Figure 2 shows the Raman spectrum for the obtained powder.

It can be seen from the figure that the given spectrum is rather complex, it has no lines typical for copper, chromium or tin sulfides. It also differs considerably from the spectra of CuCrSnS_4 spinels given in [11]. All this means the formation of a new compound.

3.2. Optical properties

Figure 3 shows the absorption spectrum of the $\text{Cu}_2\text{CrSnS}_4$ film with annealing time $t = 900$ min in Tauc coordinates.

This spectrum was obtained by re-plotting the reflection spectrum given in the insert to Fig. 3, *c* using the Kubelka–Munk equation:

$$F(R) = (1 - R)^2/2R \sim \alpha, \quad (4)$$

where R is the reflection coefficient, α is the absorption coefficient.

It can be seen from the figure that the band gap value for the $\text{Cu}_2\text{CrSnS}_4$ film is $E_g = 1.70$ eV.

Figure 4 shows the cathode luminescence spectrum for the synthesized powder, recorded at $T = 78$ K.

The maximum of this spectrum is near 1.23 eV. Based on the band gap value for the given compound, we can assume that this maximum corresponds to the donor level in the $\text{Cu}_2\text{CrSnS}_4$ zone, but its nature is not yet clear.

3.3. Photoelectrochemical measurements

Figure 5 shows the voltammogram for the $\text{Cu}_2\text{CrSnS}_4$ film with annealing time $t = 900$ min under pulsed illumination.

As seen from the figure, when light is switched on, the current density in amplitude somewhat increases, which means photosensitivity of the obtained film. Thereat, an increase in photoinduced current amplitude upon bias to the negative potential region means the *p*-type of specimen's dark conductivity [7]. The obtained voltammogram was used to estimate the specific series resistance of the obtained $\text{Cu}_2\text{CrSnS}_4$ film. It was equal to 2.30 M Ω /cm. It should be noted that the obtained values of photoinduced current and specific resistance are significantly higher than those for CZTS kesterite films usually used to make solar cells [4]. However, it is known for the same films [4] that

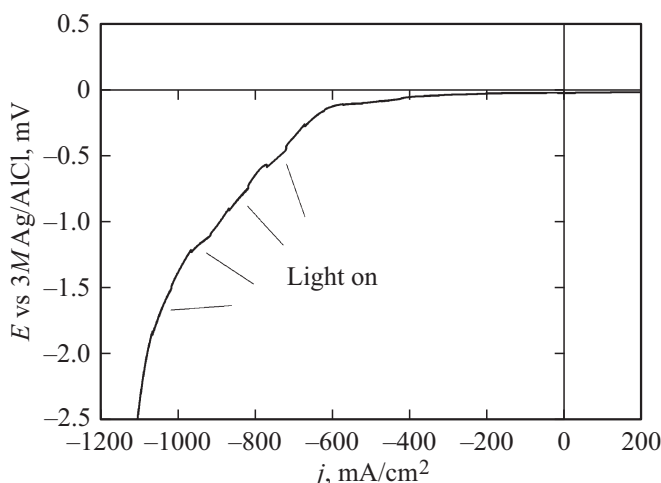


Figure 5. Voltammogram for $\text{Cu}_2\text{CrSnS}_4$ film with annealing time $t = 900$ min.

their electrophysical properties are considerably affected by stoichiometry. Therefore, the study of impact of $\text{Cu}_2\text{CrSnS}_4$ stoichiometry on optical and electrophysical properties can be a topic for further research.

4. Conclusion

Thus, microcrystalline $\text{Cu}_2\text{CrSnS}_4$ powders and films have been obtained by solid-phase synthesis for the first time. The XRD method has established that the powders have an orthorhombic structure, and determined the parameters of their crystalline lattice.

Raman spectra for microcrystalline $\text{Cu}_2\text{CrSnS}_4$ powders have been recorded for the first time.

It has been established for the first time that the band gap for microcrystalline $\text{Cu}_2\text{CrSnS}_4$ is $E_g = 1.70$ eV, and powders are characterized by a donor level in the band gap. Moreover, the obtained films are photosensitive and have the *p*-type of dark conductivity.

Funding

The work has been performed under state assignment No. AAAA-A19-119070790003-7 and No. AAAA-A19-119092390076-7.

Conflict of interest

The authors declare that they have no conflict of interest.

References

- [1] Q. Tian, Sh. Liu. *J. Mater. Chem. A*, **8**, 24920 (2020).
- [2] M.V. Gapanovich, V.V. Rakitin, G.F. Novikov. *Rus. J. Inorg. Chem.*, **67**, 3 (2022).
- [3] M.S. Kumar, S.P. Madhusudanana, S.K. Batabyal. *Sol. Energy Mater. Sol. Cells*, **185**, 287 (2018).
- [4] K. Ito. *Copper Zinc Tin Sulfide-Based Thin-Film Solar Cells* (West Sussex. UK, John Wiley and Sons Ltd, 2015).
- [5] H. Hussein, Ya. Ahmad. *Mater. Sci. Semicond. Process.*, **91**, 58 (2019).
- [6] M. Kauk, K. Muska, M. Altosaar, J. Raudoja, M. Pilvet, T. Varema, K. Timmo, O. Volobujeva. *Energy Procedia*, **10**, 197 (2011).
- [7] M.V. Gapanovich, I.N. Odin, M.V. Chukichev, V.F. Kozlovsky, G.F. Novikov. *Neorg. mater.*, **52** (1), 56 (2016) (in Russian).
- [8] S.M. Pawar, B. Pawar, A.V. Moholkar, D.S. Choi, J.H. Yun, J.H. Moon, S. Kolekar, J.H. Kim. *Electrochim. Acta*, **55**, 4057 (2010).
- [9] V.D. Das, L. Damodare. *Mater. Chem. Phys.*, **56**, 116 (1998).
- [10] S.M. Pawar, A.V. Moholkar, K.Y. Rajpure, C.H. Bhosale. *J. Phys. Chem. Solids*, **67**, 2386 (2006).
- [11] P. Valencia-Gálvez, O. Peña, S. Moris, P. Barahona. *J. Chil. Chem. Soc.*, **64**, 4285 (2019).